Microchemical Journal 142 (2018) 108–116

Contents lists available at ScienceDirect

Microchemical Journal

journal homepage: www.elsevier.com/locate/microc

Shock wave plasma generation in low pressure ambient gas from powder sample using subtarget supported micro mesh as a sample holder and its potential applications for sensitive analysis of powder samples

Javed Iqbal[a], Marincan Pardede[b], Eric Jobiliong[b], Rinda Hedwig[c], Muliadi Ramli[d], Ali Khumaeni[e], Wahyu Setia Budi[e], Nasrullah Idris[d], Syahrun Nur Abdulmadjid[d], Kurnia Lahna[d], Mangasi Alion Marpaung[f], Indra Karnadi[g], Zener Sukra Lie[c], Hery Suyanto[h], Davy Putra Kurniawan[i], Tjung Jie Lie[i], Koo Hendrik Kurniawan[i,*], Kiichiro Kagawa[i,j], May On Tjia[i,k]

[a] Department of Physics, University of Azad, Jammu & Kashmir, Muzaffarabad, Pakistan
[b] University of Pelita Harapan, 1100 M.H. Thamrin Boulevard, Lippo Village, Tangerang 15811, Indonesia
[c] Department of Computer Engineering, Bina Nusantara University, 9 K.H. Syahdan, Jakarta 14810, Indonesia
[d] Faculty of Mathematics and Natural Sciences, Syiah Kuala University, Darussalam, Banda Aceh 23111, Indonesia
[e] Faculty of Mathematics and Natural Sciences, Diponegoro University, Tembalang, Semarang 50275, Indonesia
[f] Faculty of Mathematics and Natural Sciences, Jakarta State University, 10 Rawamangun, Jakarta, Indonesia
[g] Krida Wacana Christian University, Jakarta 11470, Indonesia
[h] Faculty of Mathematics and Natural Sciences, Udayana University, Kampus Bukit Jimbaran, Denpasar 80361, Bali, Indonesia
[i] Research Center of Maju Makmur Mandiri Foundation, 40/80 Srengseng Raya, Jakarta 11630, Indonesia
[j] Fukui Science Education Academy, Takagi Chuou 2 choume, Fukui 910-0804, Japan
[k] Physics of Magnetism and Photonics Group, Faculty of Mathematics and Natural Sciences, Bandung Institute of Technology, 10 Ganesha, Bandung 40132, Indonesia

ARTICLE INFO

Keywords:
Spectrochemical analysis of powder samples
Shock wave plasma
Low pressure
LIBS
Subtarget supported micro mesh sample holder
Zn in rice

ABSTRACT

We present in this report the results of experimental study on the spectrochemical analysis of powder samples using subtarget supported micro mesh (SSMM) sample holder in low pressure ambient gases. The study is substantiated by establishing the analyte excitation mechanism with the evidence of shock wave plasma generation and the high temperature induced subsequently required for the thermal excitation and emission of the ablated atoms. The application of SSMM sample holder using Cu subtarget and stainless steel micro mesh to a number of powder samples in low pressure ambient gases are shown to produce generally sharp emission lines with low background, without suffering from intensity reduction and matrix effect commonly found in the use of pelletized powder samples. The same excellent spectral quality is demonstrated by its application to the analysis of rice samples which is the major staple diets in a large number of countries. In particular the analysis of Zn in rice is shown to exhibit a linear calibration line with extrapolated zero intercept and a detection limit of < 0.87 μg/g which is promising for quantitative analysis.

1. Introduction

The highly efficient analytical tool of laser-induced breakdown spectroscopy (LIBS) has enjoyed rapidly growing applications in the last two decades owing to its continued improvements [1–4]. In particular a large number of studies have been conducted aiming at the developments of various techniques for sample treatment and preparation in response to the great demand for rapid spectrochemical analysis of samples either found in the form of powder or bulk materials that must be pulverized into powder forms prior to the analysis [5, 6]. Among these, rice as one of the most important staple diets in Indonesia and a large number of other countries, has an urgent need for its quality assessment and control, especially concerning its content of Zn which is one of the most essential micronutrients required for the healthy growth of a child and the development of the health care of human and adult alike. More than one billion people, particularly children and pregnant women suffer from Zn deficiency related health problems in Asia [7, 8]. These pulverized powder samples are commonly mixed

* Corresponding author.
E-mail address: kurnia18@cbn.net.id (K.H. Kurniawan).

https://doi.org/10.1016/j.microc.2018.06.022
Received 10 May 2018; Received in revised form 12 June 2018; Accepted 12 June 2018

with some binding materials such as an epoxy [9–16] and pressed into pellets for laser ablation in LIBS. However, this common technique of powder sample preparation is known to give rise to the problem of matrix effect which complicates the spectral analysis [17, 18]. In addition to that, it also suffers from inevitable reduction of the analyte amount in the pelletized sample and thereby reduces the emission intensity that compromises the detection sensitivity. For that reasons, it is also inapplicable to cases with limited amount of available powder sample.

An alternative method of handling powder sample was introduced in 2007 by trapping the powder in a quartz subtarget having a random distribution of micro holes on its surface [19]. The micro holes were fabricated with diamond powder of 30 μm diameter which resulted in micro holes of roughly 30 μm diameter and 30 μm depth on the quartz surface. The powder sample was then pulverized to the sizes of about 30 μm or less so that they could be trapped on the quartz surface without being blown away by the laser pulses. This was found to work out fine, showing no observable amount of the powder loss due to the laser ablation nor detectable interfering emission from the subtarget. Nevertheless the sample holder is expensive and inpracticable to make.

In a recently published work [20], another still simpler alternative was introduced utilizing a special powder sample holder made of Cu subtarget supported micro mesh (SSMM). The powder is evenly spread to cover the mesh and gently pressed to form a firm powder layer of appropriate hardness and thickness needed to generate the desired plasma emission. It was shown that sensitive plasma emission of excellent spectral quality was obtained virtually free from background interference. It was also shown that the plasma emission characteristics indicated the role of shock wave plasma induced thermal excitation process. Further measurement on a number of the standard soil samples of various Pb contents were shown to yield a linear calibration line with practically zero intercept and a detection limit of < 10 ppm. Despite the favorable results reported in the previous studies [19, 20], the generation of shock wave plasma was only indicated by the plasma emission characteristics, leaving its direct detection and the underlying plasma excitation mechanism less than appropriately addressed.

This study is undertaken to demonstrate the usefulness of LIBS analysis of powder sample using the SSMM sample holder in low pressure ambient gases. It is also substantiated on the one hand by providing a direct evidence on the generation of shock wave plasma from a Cu powder sample for the thermal excitation required in LIBS. On the other hand, it is corroborated by the excellent spectra featuring sharp emission lines and low background obtained from a variety of powder samples measured by the proposed experiment setup. Further, the viability of SSMM powder sample holder is demonstrated by the excellent emission spectra of rice samples, exhibiting a linear calibration line with zero intercept for Zn analysis in rice with a low detection limit of < 1 ppm.

2. Experimental procedure

The experimental setup for density jump measurement is shown in Fig. 1(a) which was used in a previous experiment [21–23]. The plasma emission is imaged 1:1 by a quartz lens (L_2) of $f = 150$ mm onto the entrance plane of the monochromator (SPEX M-750, Czerny-Turner configuration, focal length 750 mm with 1200 grooves mm^{-1} blazed at 500 nm) where it is detected by a photomultiplier (Hamamatsu IP-28) from which the electrical signal is fed through a fast preamplifier into the first channel of a digital sampling storage scope. The sampling storage scope is triggered by the synchronized external trigger signal from the laser system for the timely reading of the appearance of the plasma emission. At the same time, the direct detection of the plasma front arrival is carried out by an optical interferometric method. It should be pointed out that the density jump signal is not related with the mechanical impact caused by the sudden arrival of the plasma mass flow. Instead it is an optical signal detected as a sudden change in the interference pattern brought about by the arrival of the shock wave plasma as explain below. For that purpose, a He-Ne laser is used as a probe beam and directed by means of a mirror (M_1) through the plasma expansion region in the chamber. The outgoing probe beam is then sent via another mirror (M_2) into the cylindrical glass of diameter 60 mm (L_3), where all but the central rays are slightly deviated from the incoming beam direction. These spread out rays are reconverged by the cylindrical glass producing interference fringes of highest visibility on the entrance slit (20 μm wide) of PMT (Hamamatsu R1104) by the proper adjustment of the M_2 mirror. The filter behind the slit and the PMT are arranged to detect the dark area between the first two bright fringes. The separation between adjacent fringes in the absence of laser plasma is about 0.1 mm on the PMT entrance slit which is 80 cm away from the cylindrical glass. A phase change is bound to take place in the He-Ne probe beam caused by the corresponding change of refractive index in the medium upon the arrival of shock wave plasma front. Consequently this will shift the fringe pattern and move the 2nd bright fringe into the detector window to produce the density jump signal marked by the sudden appearance of the bright optical fringe. The associated electric signal from the PMT is fed into the second channel of the digital sampling storage scope. The density jump signal is recorded and displayed on the screen of the oscilloscope as a dip upon the arrival time of the shock wave front in coincidence with the recording of the plasma emission in the first-channel of the oscilloscope. A vertical slit which is placed in front of the PMT (Hamamatsu R1104) is used to avoid disturbances from unwanted stray light including that from the primary plasma which is further blocked by an interference filter for He-Ne laser wavelength place behind the slit. For the measurement of the plasma front propagation, the density jump measurement described above is repeated successively at the different plasma position (effectively the chamber position) which is moved step wise farther away from the He-Ne laser light.

The schematic diagram of the experimental setup for spectroscopic measurement is given by Fig. 1(b) along with the inset describing the SSMM sample holder which was fabricated and employed in a previous experiment [20], for which a Cu plate of 99.9% purity from Rare Metallic Co. is used as the subtarget along with a stainless steel mesh as the powder sample holder. It is confirmed that no Cu emission line from the Cu plate nor Fe emission line from the stainless steel mesh are found in a separate preliminary experiment using the standard KBr sample (purity 5 N) purchased from Rare Metallic. Hence its use is not expected to interfere with and complicate the detected analyte spectrum in the spectral range from 250 to 600 nm. The laser used in this experiment is a nano-second (ns) Nd:YAG laser (Quanta Ray, Lab Series, 450 mJ, 1064 nm, 8 ns) operated in Q switched mode at 10 Hz repetition rate and a reduced output energy of 68 mJ. The laser beam is directed onto the sample in the chamber through a quartz window of the chamber. A convex lens of 150 mm focal length is used with -5 mm defocused condition to yield a power density of around 200 MW/cm^2 on the sample surface. The choices of the laser energy and focusing condition are determined in another preliminary experiment searching for the minimum ablation power density needed to yield stable and reproducible analyte intensities from the powder sample without inducing the Cu and Fe emission lines from the sample holder and causing blowing-off of the sample powder in a low pressure ambient gas. The chamber is equipped with an inlet and outlet ports for the continuous flow of ambient gas at a constant flow-rate to maintain the gas pressure at 30 Torr. The chamber has an additional quartz window for the observation of plasma emission. The plasma emission intensity is collected at one end of an optical fiber of 10 μm core diameter, with its other end connected to the entrance slit of an Echelle spectrograph (Mechelle M500 type equipped with a gated ICCD system, Andor iStar ICCD, 200–975 nm wavelength) for the measurement of emission spectrum in a broad spectral range.

For the search and verification of the existence of calibration line, a spectrograph (McPherson model 2061 with 1 m focal length, 1800 g/

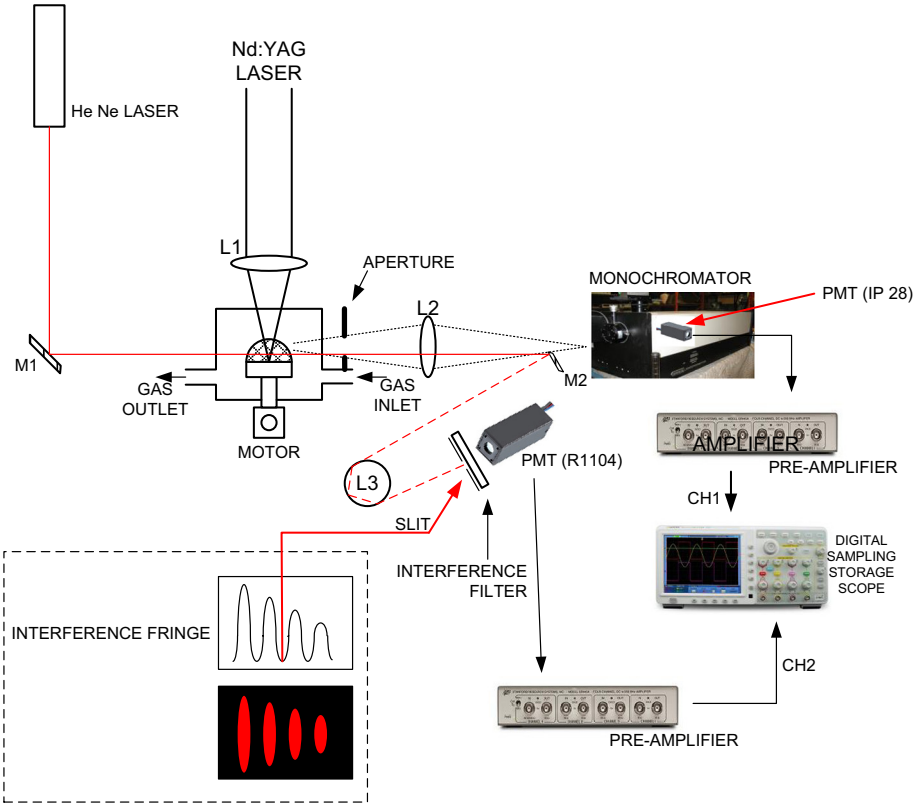

(a)

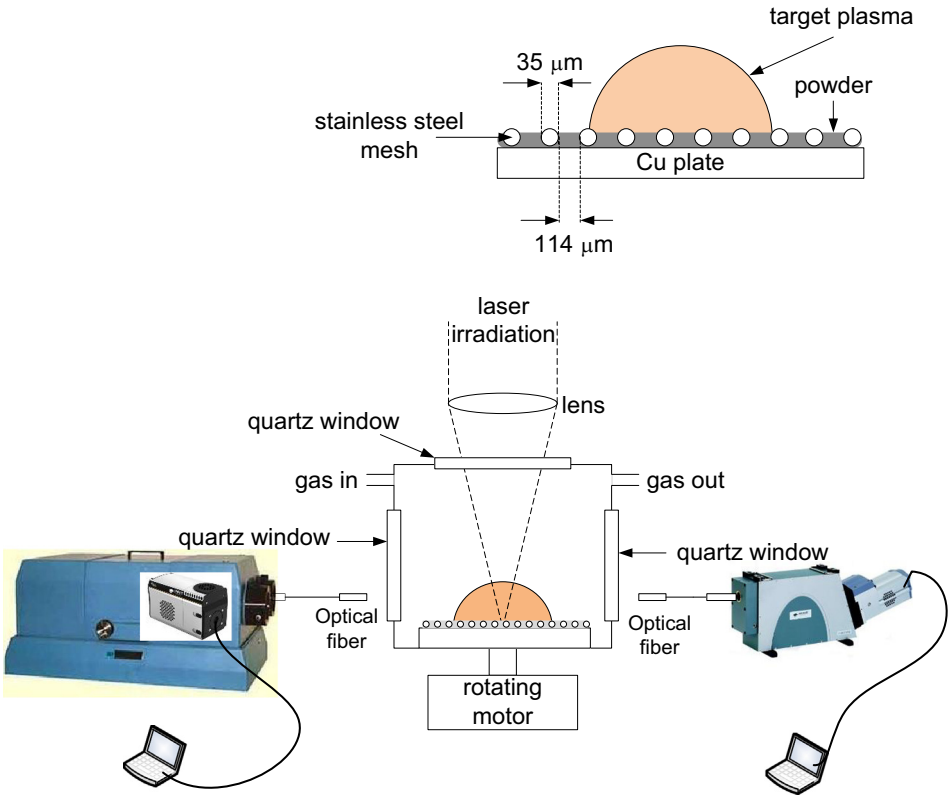

(b)

Fig. 1. Diagram of the experimental setup; (a) for measuring the density jump measurement and (b) for measuring the emission spectra of the powder sample.

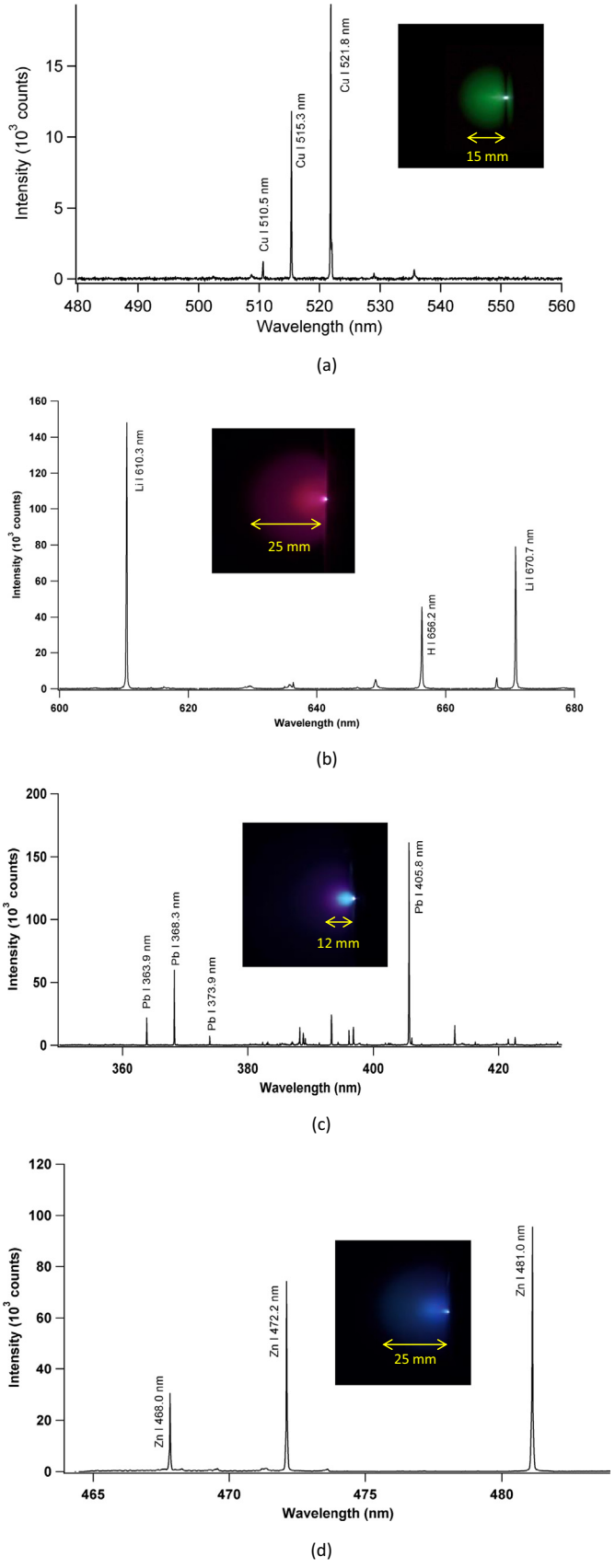

Fig. 2. Photograph of the plasma and its related spectra generated by 68 mJ laser irradiation focused under −5 mm defocused condition on the different kinds of powder samples in He ambient gas at 2 kPa; (a) $CuSO_4$ powder, (b) LiF powder, (c) $PbCl_2$ powder and (d) ZnS powder.

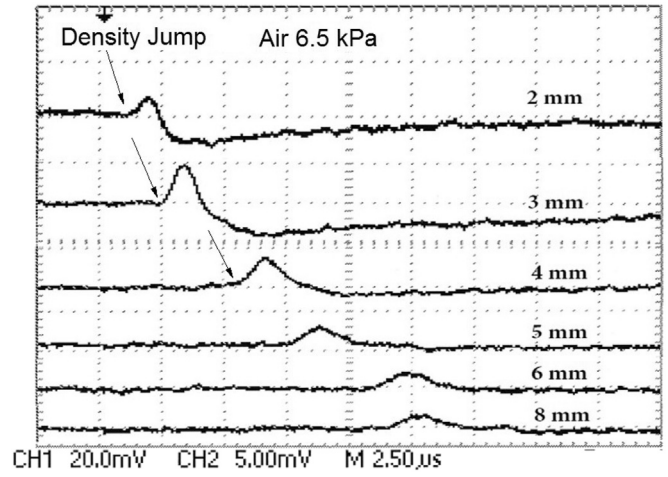

Fig. 3. The density jump signal recorded by the oscilloscope at the different probing position. The laser pulses of 68 mJ is focused under −5 mm defocused condition on the $CuSO_4$ powder sample in low pressure air ambient gas at 6.5 kPa.

mm grating and f/8.6 Czerny Turner configuration) is employed with its exit slit attached to a gated ICCD system (Andor I*Star intensified CCD 1024 × 256 pixels) as described in by the left-hand branch of the detection system in Fig. 1(b). The samples used in this experiment consist of powder samples of $CuSO_4$, LiF, $PbCl_2$, ZnS, sucrose, $MgCO_3$, $Al(OH)_3$, obtained from Rare Metallic Co. The rice samples used in this part of experiment are those containing Zn impurity at varied contents of 0.312%, 0.625%, 1.25%, 2.5% and 5%. All the powder samples are pulverized into the grain sizes of < 50 µm. The samples are rotated during the measurement so that each laser pulse will hit a different spot on the sample surface. The resulted data from 30 laser shots from each sample are then averaged over the data from all spots and presented as the data points (intensity) of the sample with the corresponding Zn content.

3. Results and discussion

3.1. Excitation mechanism of the powder sample plasma

Prior to the main experiment, a preliminary visual inspection is conducted on the plasma generated in 2 kPa He ambient gas by 68 mJ laser pulses directed under −5 mm defocused condition onto the powder samples of (a) $CuSO_4$; (b) LiF; (c) $PbCl_2$; (d) ZnS. The resulted plasmas and its related spectra shown in Fig. 2 are found to exhibit a typical hemispherical shape consisting of a small and intense primary plasma and an extended secondary plasma growing out of the primary plasma as observed previously [24–39]. The relatively tiny primary plasma generally shows very dense white colour originating from the intense continuum emission, while the much larger secondary plasmas extending far beyond the primary plasma reaching a maximum radius of around 25 mm and displays the bright colours of the emission from the associated constituents. For comparison, we recall that in the case of LIBS employing atmospheric ambient air, one usually observes a very dense plasma of much smaller size (< 3 mm) exhibiting a bright white colour associated mostly with the strong continuum emission of the sample. The colour of the secondary plasma shown in Fig. 2 varies with the host elements of the sample. For $CuSO_4$ powder, the colour appears green as it is composed of the Cu I 510.5 nm, Cu I 515.3 nm and Cu I 521.8 nm emission lines. The plasma colour appears red for LiF powder as it is composed of the Li I 610.3 nm and Li I 670.7 nm emission lines. For $PbCl_2$ powder, the plasma colour appears redish blue being composed of the Pb I 405.7 nm and Cl I 837.5 nm emission lines. The plasma colour is magenta for ZnS powder, associated with the Zn I 468.0 nm,

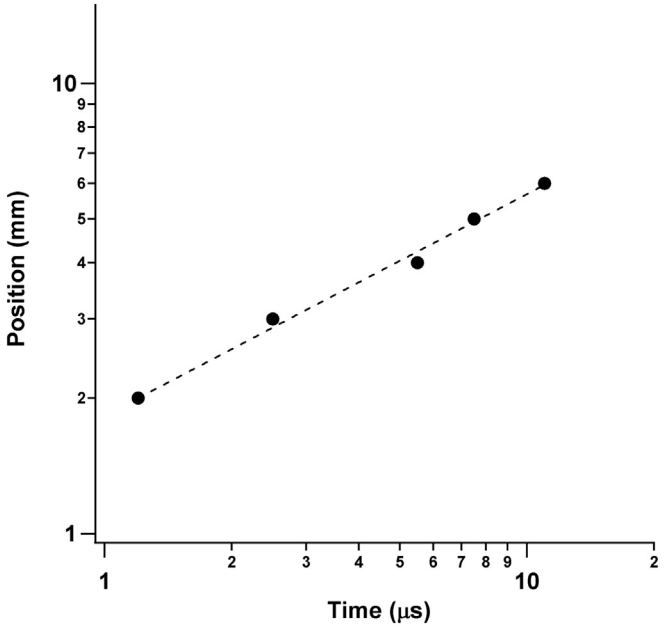

Fig. 4. Propagation length of the arrival of the density jump at different plasma positions.

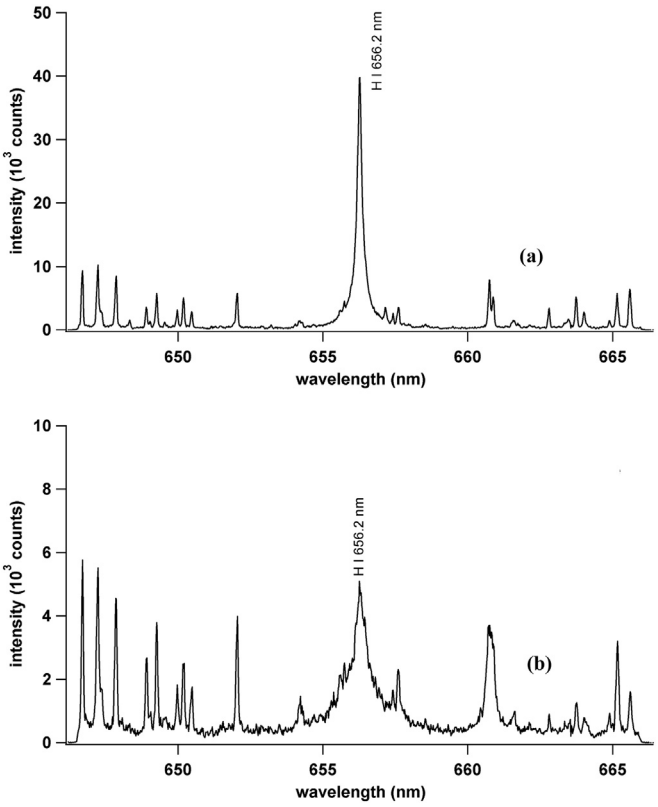

Fig. 5. Emission spectra of H I 656.2 nm taken from wet mud painted on the mesh surface. The laser pulses of 68 mJ is focused under −5 mm defocused condition on the $CuSO_4$ powder sample in low pressure He ambient gas at 5 kPa.

Zn I 472.2 nm and Zn I 481.0 nm emission lines. It is also interesting to note that the faint orange colour appearing in the outermost layer of all the secondary plasmas has its origin from the He I 587.6 nm emission line.

The shadowgraph measurement of the shock wave plasma propagation is performed with 68 mJ laser pulses focused on the $CuSO_4$ powder sample in low pressure ambient air at 6.5 kPa, The result presented in Fig. 3 displays the density jump signal recorded by the oscilloscope as a clear deflection from the probing He-Ne laser background. This signal is associated with the spatial shift of the spectral fringes arising from the arrival of the plasma front as explained earlier. The times (t) of the appearance of these signals and the corresponding positions of its detection measured by the chamber position are plotted in Fig. 4 for the verification of a shock wave characteristic according to the Sedov criterion given below,

$$r = (E_0/\alpha\,\rho)^{1/5}\, t^{2/5}$$

where r is the radius of the hemispherical plasma front marked by the detected density jump position, t is the time measured from the start of the explosion, ρ is the gas density, α is the constant involving the specific heats of the gas and E_0 is the initial explosion energy. Except for

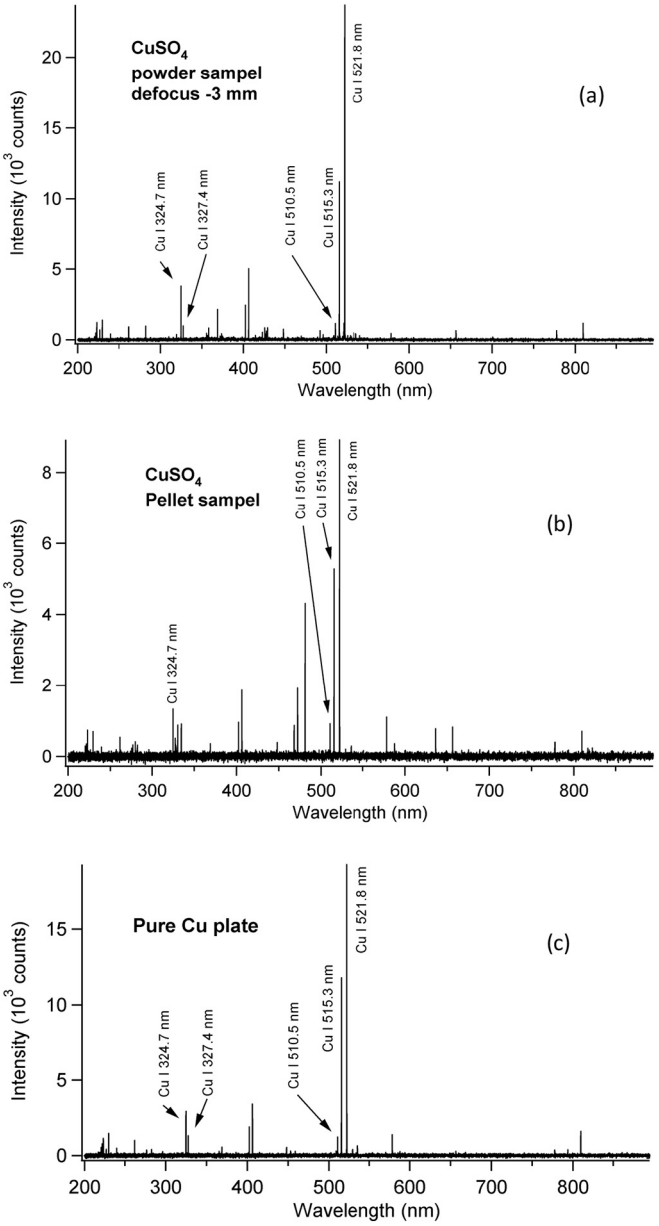

Fig. 6. Emission spectra of (a) $CuSO_4$ powder painted on the mesh surface, (b) $CuSO_4$ pellet and (c) pure Cu plate in He ambient gas at 5 kPa. The laser irradiation is focused under −5 mm defocused condition in case (a) and tight focused condition in cases (b) and (c).

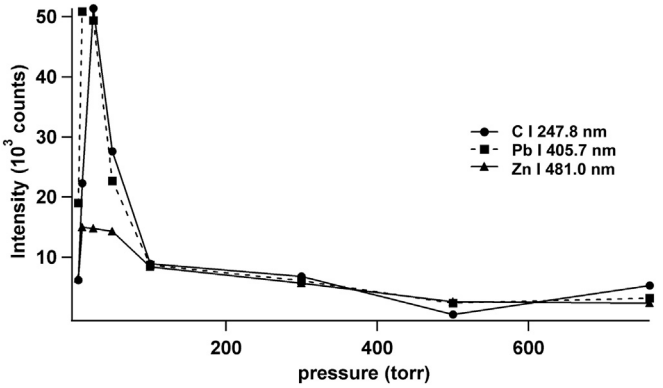

Fig. 7. Pressure dependent emission intensity of C I 247.8 nm, Zn I 481.0 nm and Pb I 405.7 nm in He gas. Powder mixture of $PbCl_2$ + sucrose + ZnS is used as a sample. The laser pulses of 68 mJ is focused under −5 mm defocused condition on the powder mixture.

r and t, all the other quantities are determined by the experimental condition and using the available standard data for air [40]. It is shown that the plot is nicely fitted by a straight line (with $R^2 = 0{,}99$) with a slope of 0.4, in good agreement with the speed of shock wave induced by a point explosion [40]. This result therefore confirms the generation of shock wave plasma from the powder sample using the SSMM sample holder, which is supposed to be responsible for the thermal excitation of the ablated atoms as further described below.

The thermal excitation process induced by the shock wave plasma is indicated by the plasma temperature, particularly at the plasma front. In order to determine the plasma temperature using the standard two line method, it is necessary to estimate the electron density in the plasma. This is performed by using a mud sample (containing high concentration of hydrogen) which is dried in room temperature of 25 °C as long as it is needed to reduce the water concentration to around 15%. Then the mud is painted on the surface of the mesh and irradiated with the 68 mJ laser light under −5 mm defocused condition. The resulted spectra is presented in Fig. 5, (a) in 5 kPa He gas and (b) 101 kPa He gas. Based on the FWHM of the H I 656.2 nm emission line, the electron densities of the plasmas are estimated around 10^{17} and 10^{19} for the low pressure and atmospheric pressure He gases. One may therefore assumed the existence of local thermal equillibrium (LTE) condition for the application of the two-lines method. The plasma temperature of around 9000 K is estimated from the intensity ratio of the Cu I 521.8 nm and Cu I 510.5 nm emission lines in Fig. 6(a), assuming Boltzmann distribution law in the plasma. This temperature indicates the effective conversion from the kinetic energy of the shock wave plasma to the thermal energy for the needed excitation of the ablated atoms as explained previously [24–39].

3.2. Analytical application of other powder samples

Before turning to the discussion of analytical application of powder samples using SSMM powder sample holder, one needs to address the following important issues. Firstly, it must be verified that no ablation takes place on the copper subtarget and the stainless steel mesh. Further, it should be assured that no significant amount of the powder sample is lost during the laser ablation process. These issues are dealt with in an experiment employing $CuSO_4$ powder sample by (a) using the SSMM powder sample holder, (b) pelletizing the powder and (c) using a Cu plate sample. The same 68 mJ laser irradiation is employed in all three cases with the laser beam −5 mm defocused in case (a), but tightly focused for (b) and (c) cases. The result is presented in Fig. 6. One clearly sees that the emission spectra of Fig. 6(a) and (c) exhibit closely similar intensity distribution without extra contributions from the Cu subtarget and the stainless steel mesh. Besides, no significant intensity reduction is shown in Fig. 6(a), implying no significant loss of powder caused by the laser ablation. A microscopic observation of the sample holder after the laser irradiation also fails to show any sign of damage on the Cu plate used as a subtarget. On the other hand, comparison of Fig. 6(a) and (b) clearly shows significant intensity reduction in addition to the matrix effect marked by the appearance of the binding material emission lines in the case of pelletized powder sample.

Given the excellent spectrum shown in Fig. 6(a), it is tempting to examine the possibility of performing quantitative powder analysis using the SSMM sample holder. In view of the sensitive pressure dependence emission intensity reported previously report [24–39], it is important to determine the optimum ambient gas pressure for the choice of the ambient gas pressure. This pressure dependent variation of the emission intensity is performed on a mixture of $PbCl_2$, sucrose and ZnS, which is expected to provide information on the pressure dependent intensity variations of the light element represented by C; and the moderate and heavier weight elements, represented by Zn and Pb, respectively. Fig. 7 displays the resulted pressure dependent emission intensities measured in He gas using 68 mJ laser irradiation under −5 mm defocused condition. It is clear that the maximum emission intensities for all the elements (C, Zn and Pb) are obtained around 5 kPa and this is the gas pressure applied in the following measurements.

The viability of SSMM powder sample holder is further examined by its application to analyses of Mg and Ca health supplements in He ambient gas. The measured spectra presented in Fig. 8 show the appearance of strong and sharp C, Ca and Mg emission lines with very low background beside the equally sharp He I 587.6 nm and He I 667.8 nm emission lines from the He ambient gas. Recalling the reported role of He ambient gas in the enhancement of the emission intensity of the ablated atoms [24, 25], it is worthwhile to repeat the measurement of a mixture of HBO_3, $MgCO_3$, ZnS, $CaCO_3$, Al_2O_3, $Fe(OH)_3$, $CuSO_4$, $MnCO_3$, LiF in ambient air at reduced pressure of 0.65 kPa to investigate the real need of using He ambient gas. The resulted emission spectrum given in

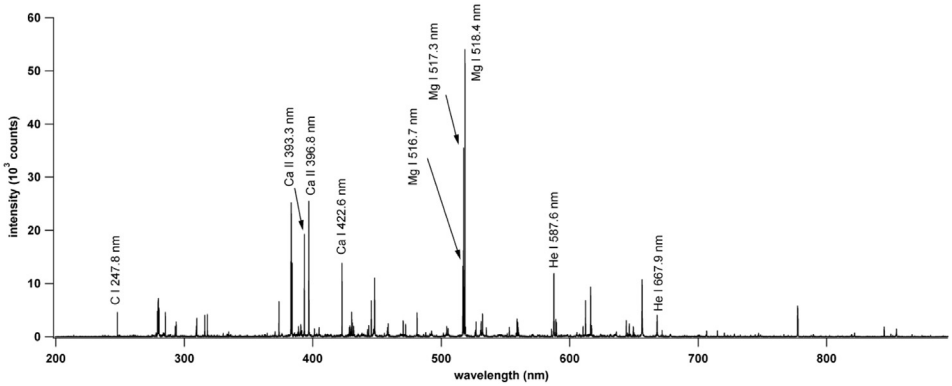

Fig. 8. Emission spectra of health supplement containing Mg and Ca. The laser pulses of 68 mJ is focused under −5 mm defocused condition on the powder mixture.

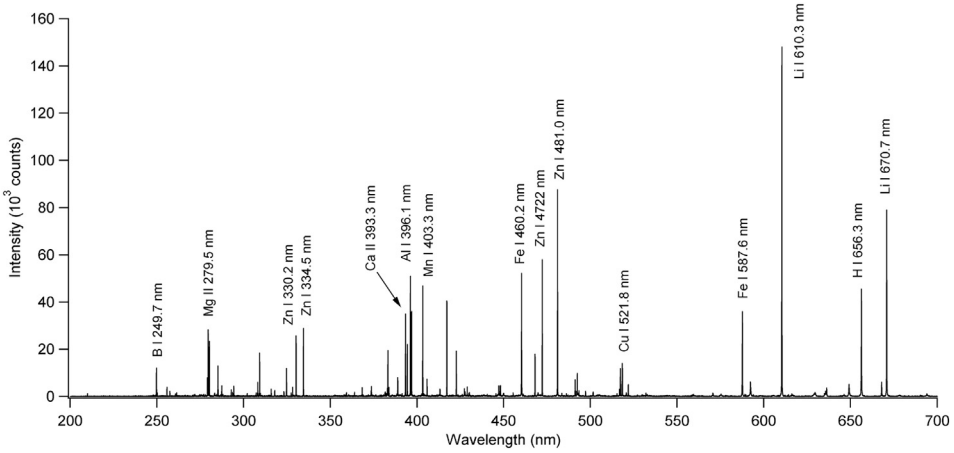

Fig. 9. Emission spectra of mix powder sample containing HBO_3, $MgCO_3$, ZnS, $CaCO_3$, Al_2O_3, $Fe(OH)_3$, $CuSO_4$, $MnCO_3$, LiF. The laser pulses of 68 mJ is focused under −5 mm defocused condition on the powder mixture.

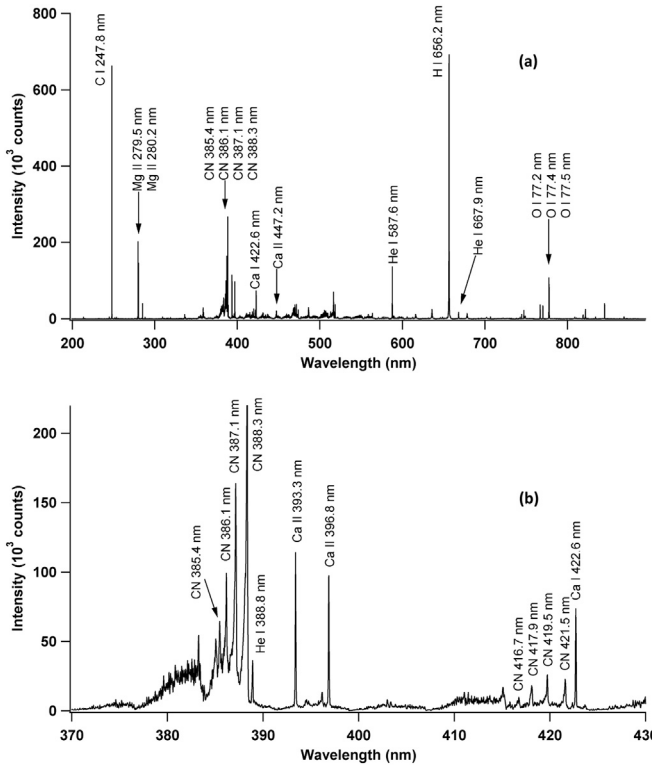

Fig. 10. Emission spectra of Indonesian rice (a) in the wavelength region of 200–850 nm and (b) zoom region of 370–430 nm. The laser pulses of 68 mJ is focused under −5 mm defocused condition on the powder mixture.

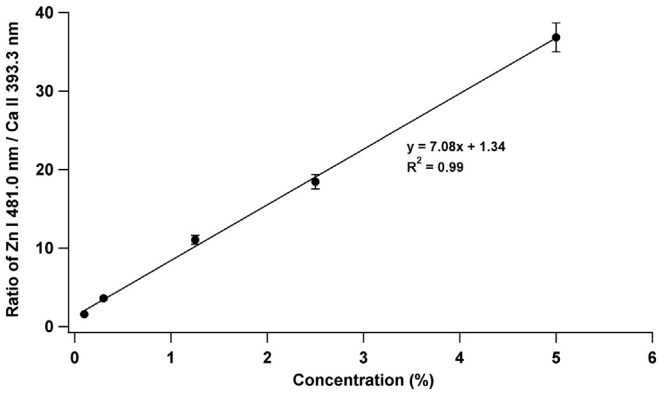

Fig. 11. Calibration line of Zn I 481.0 nm/Ca II 393.3 nm in Indonesian rice. The laser pulses of 68 mJ is focused under −5 mm defocused condition on the powder mixture.

Fig. 9 clearly exhibits strong and sharp emission lines of all the relevant elements with low background. This shows that low pressure ambient air can be used for comparable results instead of the more expensive He gas.

The excellent spectra quality displayed in Figs. 8 and 9 suggests the possibility of performing quantitative analysis of powder sample. Indonesian red rice has come as a natural choice of sample in this experiment as it has become a favorite choice for its lower carbohydrate content. The rice is pulverized to the grain size of < 50 μm and then deposited in the SSMM sample holder. The result of the same measurement on the rice sample in He ambient gas is shown in Fig. 10 for (a) the wavelength region of 200–900 nm and (b) the zoomed wavelength region of 370–430 nm, where all the well known C, Mg, Ca, H, O emission lines and the CN emission band are clearly detected along with He emission.

A further investigation of the possibility for quantitative analysis is focused on the Zn impurity in rice for the reason mentioned in the introductory section. This is conducted by repeating the same measurement of emission intensities of the rice samples provided by the supplier with different Zn contents. Each data point in this figure is the average of 30 data produced by 30 successive laser shots on the rotating SSMM sample holder. The measurement is repeated on five different radial positions on the same sample surface show highly reproducible results implying the high uniformity of Zn distribution in the sample. The measured Zn I 481.0 nm intensities normalized by the nearby Ca II 393.3 nm emission intensity are plotted versus the associated Zn contents in Fig. 11. The result is seen to exhibit a nice linear relationship having extrapolated zero intercept. The limit of Zn detection is estimated from the emission spectrum of the rice sample containing 0.12% Zn impurity shown in Fig. 12, and obtained by following the conventional criterion as a ratio of the signal intensity against three times the average surrounding background intensity. The resulted detection limit is found to be < 0.87 μg/g which is more than adequate for the common criterion of several tens μg/g adopted in quality assessment of rice.

4. Conclusion

This study has demonstrated the successful application of copper subtarget supported stainless steel micro mesh (SSMM) powder sample holder for the generation of shock wave plasma in low pressure ambient

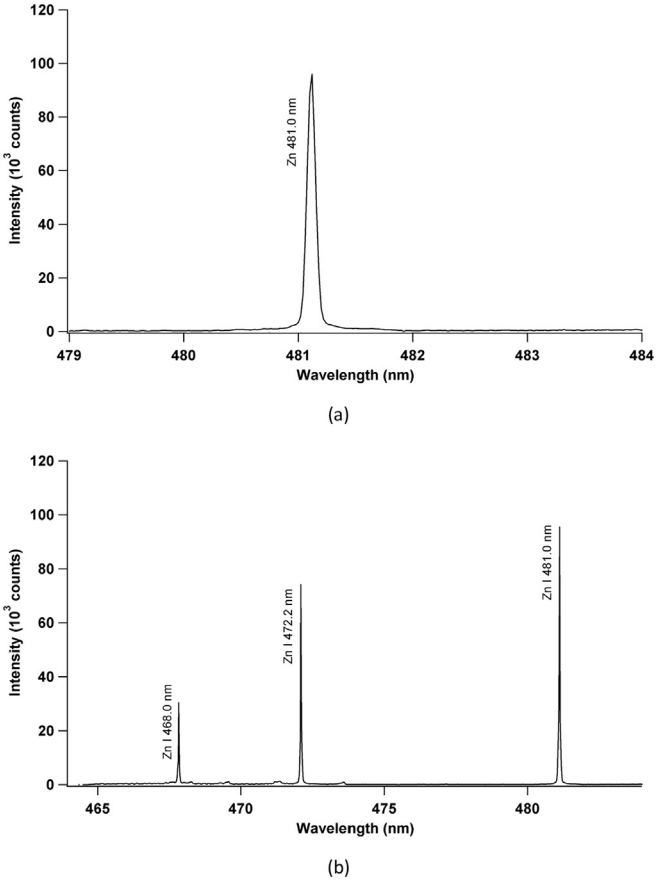

Fig. 12. Emission spectra of Zn I 481.0 nm ((a), zoom region) taken from Fig. 11 which containing 0.12% Zn and (b) wide range spectra. The laser pulses of 68 mJ is focused under −5 mm defocused condition on the powder mixture.

gas and its induced high temperature responsible for thermal excitation of the ablated atoms. The results further exhibit the excellent emission spectra produced from powder samples by laser irradiation in low pressure ambient air and He gas. It is shown that no powder loss is found during the laser ablation process hence no intensity reduction is detected as commonly observed from pelletized powder samples. Besides, it is also free from matrix effect as invariably encountered in the use of pelletized powder samples. Further experiment with rice sample containing various Zn contents has resulted in a linear calibration line with extrapolated zero intercept and detection limit of $< 0.87\ \mu g/g$ which is promising for quantitative analysis of Zn in rice.

Acknowledgement

This work was partially supported through a Basic Research Grant in Physics, The Academy of Sciences for the Developing World, Third World Academy of Sciences (TWAS), under contract no. 060150 RG/PHYS/AS/UNESCO FR:3240144882. This work was also partially supported through Visiting Expert Programme, The Academy of Sciences for the Developing World, Third World Academy of Sciences (TWAS), under contract No. F.R. 3240294906.

References

[1] D. Paules, S. Hamida, R.J. Lasheras, M. Escudero, D. Benouali, J.O. Caceres, J. Anzano, Characterization of natural and treated diatomite by Laser-Induced Breakdown Spectroscopy (LIBS), Microchem. J. 137 (2018) 1–7.
[2] K. Song, Y.I. Lee, J. Sneddon, Applications of laser-induced breakdown spectroscopy, Appl. Spectrosc. Rev. 32 (1997) 183–235.
[3] A.C. Ranulfi, G.S. Senesi, J.B. Caetano, M.C. Meyer, A.B. Magalhaes, P.R. Villas-Boes, D.M.B.P. Milori, Nutritional characterization of healthy and *Aphelenchoides besseyi* infected soybean leaves by Laser-Induced Breakdown Spectroscopy (LIBS), Microchem. J. 141 (2018) 118–126.
[4] Y. Li, D. Tran, Y. Ding, G. Yang, K. Liu, C. Wang, X. Han, A review of laser-induced breakdown spectroscopy signal enhancement, Appl. Spectrosc. Rev. 53 (2018) 1–35.
[5] S.C. Jantzi, V. Motto-Ros, F. Trichard, Y. Markushin, N. Melikechi, A. De Giacomo, Sample treatment and preparation for laser-induced breakdown spectroscopy, Spectrochim. Acta B 115 (2016) 52–63.
[6] J. Sneddon, Advances in Atomic Spectroscopy, JAI Press Inc., Stamford, Connecticut, US, 1999.
[7] B.P. Mallikarjuna Swamy, M.A. Rahman, M.A. Inabangan-Asilo, A. Amparado, C. Manito, P.C. Mohanty, R. Reinke, I.H. Slamet-Loedin, Advances in breeding for high grain zinc in rice, Rice (2016), http://dx.doi.org/10.1186/s12284-016-0122-5.
[8] H. Rehman, T. Aziz, M. Farooq, A. Wakeel, Z. Rengel, Zinc nutrition in rice production systems: a review, Plant Soil 361 (2012) 203–226.
[9] B. Lal, H. Zheng, F.Y. Yueh, J.P. Singh, Parametric study of pellets for elemental analysis with laser-induced breakdown spectroscopy, Appl. Opt. 43 (2004) 2792–2797.
[10] P. Musil, V. Otruba, V. Kanicky, J.M. Mermet, Determination of elements in agricultural soil using infra-red laser ablation inductively coupled plasma – atomic emission spectrometry, Spectrochim. Acta B 55 (2000) 1747–1758.
[11] G.S. Senesi, M. Deli'Aglio, R. Gaudiuso, A. De Giacomo, C. Zaccone, O. De Pascale, T.M. Miano, M. Capitelli, Heavy metal concentrations in soils as determined by laser-induced breakdown spectroscopy (LIBS), with special emphasis on chromium, Environ. Res. 100 (2009) 413–420.
[12] A.M. Popov, T.A. Labutin, S.M. Zaytsev, I.V. Seliverstova, N.B. Zorov, I.A. Kal'Ko, Y.N. Sidorina, I.A. Bugaev, Y.N. Nikolaev, Determination of Ag, Cu, Mo and Pb in soils and ores by laser-induced breakdown spectrometry, J. Anal. At. Spectrom. 29 (2014) 1925–1933.
[13] M. Hassan, M. Sighicelli, A. Lai, F. Colao, A.H. Hanafy Ahmed, R. Fantoni, M.A. Harith, Studying the enhanced phytoremediation of lead contaminated soils via laser induced breakdown spectroscopy, Spectrochim. Acta B 63 (2008) 1225–1229.
[14] J.J. Choi, S.J. Choi, J.J. Yoh, Standoff detection of geological samples of metal, rock, and soil at low pressures using laser-induced breakdown spectroscopy, Appl. Spectrosc. 70 (2016) 1411–1419 (DOI 0003702816664858).
[15] S.C. Yao, J.L. Xu, X. Dong, B. Zhang, J.P. Zheng, J.D. Lu, Optimization of laser-induced breakdown spectroscopy for coal powder analysis with different particle flow diameters, Spectrochim. Acta B 110 (2016) 146–150.
[16] W.Q. Lei, J. El Haddad, V. Motto-Ros, N. Gilon-Delepine, A. Stankova, Q.L. Ma, X.S. Bai, L.J. Zheng, H.P. Zeng, J. Yu, Comparative measurements of mineral elements in milk powders with laser-induced breakdown spectroscopy and inductively coupled plasma atomic emission spectroscopy, Anal. Bioanal. Chem. 400 (2011) 3303–3313.
[17] A.S. Eppler, D.A. Cremers, D.D. Hickmott, M.J. Ferris, A.J. Koskelo, Matrix effects in the detection of Pb and Ba in soils using laser-induced breakdown spectroscopy, Appl. Spectrosc. 50 (1996) 1175–1181.
[18] J.M. Anzano, M.A. Villoria, A. Ruiz-Medina, R.J. Lasheras, Laser-induced breakdown spectroscopy for quantitative spectrochemical analysis of geological materials: effects of the matrix and simultaneous determination, Anal. Chim. Acta 575 (2006) 230–235.
[19] Z.S. Lie, M. Pardede, R. Hedwig, M.M. Suliyanti, K.H. Kurniawan, Munadi, Y.I. Lee, K. Kagawa, I. Hattori, M.O. Tjia, Spectrochemical analysis of powder using 355 nm Nd-YAG laser-induced low pressure plasma, Anal. Bioanal. Chem. 390 (2008) 1781–1787.
[20] H. Suyanto, T.J. Lie, K.H. Kurniawan, K. Kagawa, M.O. Tjia, Practical soil analysis by laser induced breakdown spectroscopy employing subtarget supported micro mesh as a powder sample holder, Spectrochim. Acta B 137 (2017) 59–63.
[21] K.H. Kurniawan, T.J. Lie, N. Idris, M.O. Tjia, M. Ueda, K. Kagawa, Detection of the density jump in the laser-induced shock wave plasma using low energy Nd:YAG laser at low pressures of air, J. Spectroscs. Soc. Jap. 50 (2001) 13–18.
[22] K.H. Kurniawan, K. Lahna, T.J. Lie, K. Kagawa, M.O. Tjia, Detection of density jump in laser-induced shock wave plasma using a rainbow refractometer, Appl. Spectrosc. 55 (2001) 92–97.
[23] K. Lahna, M. Pardede, K.H. Kurniawan, K. Kagawa, M.O. Tjia, Direct evidence of laser-induced shock wave plasma from organic targets in low pressure He ambient gas, showing the effect of target hardness on its propagation speed and the resulted spectral performance, Appl. Opt. 57 (2017) 9876–9881.
[24] K.H. Kurniawan, K. Kagawa, Hydrogen and deuterium analysis using laser-induced plasma spectroscopy, Appl. Spectrosc. Rev. 41 (2006) 99–130.
[25] K.H. Kurniawan, M.O. Tjia, K. Kagawa, Review of laser-induced plasma, its mechanism, and application to quantitative analysis of hydrogen and deuterium, Appl. Spectrosc. Rev. 49 (2014) 323–434.
[26] N. Idris, K.H. Kurniawan, T.J. Lie, M. Pardede, H. Suyanto, R. Hedwig, T. Kobayashi, K. Kagawa, T. Maruyama, Characteristics of hydrogen emission in laser plasma induced by focusing fundamental Q-sw YAG laser on solid samples, Jpn. J. Appl. Phys. 43 (2004) 4221–4228.
[27] K.H. Kurniawan, W. Setia Budi, M.M. Suliyanti, A.M. Marpaung, K. Kagawa, Characteristics of laser plasma induced by a irradiation of a normal oscillation YAG laser at low pressures, J. Phys. D. Appl. Phys. 30 (1997) 3335–3345.
[28] W. Setia Budi, W. Tjahyo Baskoro, M. Pardede, K.H. Kurniawan, M.O. Tjia, K. Kagawa, Neutral and ionic emission in Q-sw Nd-YAG laser induced shock wave plasma, Appl. Spectrosc. 53 (1999) 1347–1351.
[29] M. Pardede, K.H. Kurniawan, M.O. Tjia, K. Ikezawa, T. Maruyama, K. Kagawa,

Spectrochemical analysis of metal elements electrodeposited from water sample by laser induced shock wave plasma spectroscopy, Appl. Spectrosc. 55 (2001) 1229–1236.
[30] K.H. Kurniawan, T.J. Lie, K. Kagawa, M.O. Tjia, Laser-induced shock wave plasma spectrometry using a small chamber designed for in situ analysis, Spectrochim. Acta B 55 (2000) 839–848.
[31] K. Kagawa, T.J. Lie, R. Hedwig, S.N. Abdulmadjid, M.M. Suliyanti, K. Kagawa, Subtarget effect on laser plasma generated by transversely excited atmospheric CO_2 laser at atmospheric gas pressures, Jpn. J. Appl. Phys. 39 (2000) 2643–2646.
[32] M.M. Suliyanti, S. Sardy, A. Kusnowo, M. Pardede, R. Hedwig, K.H. Kurniawan, T.J. Lie, D.P. Kurniawan, K. Kagawa, Preliminary analysis of C and H in a Sangiran fossil using laser-induced plasma at reduced pressure, J. Appl. Phys. 98 (093307) (2005) 1–8.
[33] K.H. Kurniawan, T. Kobayashi, S. Nakajima, K. Kagawa, Correlation between the front speed and initial explosion energy of the blast wave induced by a TEA CO_2 laser, Jpn. J. Appl. Phys. 31 (1992) 1213–1214.
[34] M. Ramli, N. Idris, K. Fukumoto, H. Niki, F. Sakan, T. Maruyama, K.H. Kurniawan, T.J. Lie, K. Kagawa, Hydrogen analysis in solid samples by utilizing He metastable atoms induced by TEA CO_2 laser plasma in helium gas at 1 atmosphere, Spectrochim. Acta B 62 (2007) 1379–1389.
[35] K.H. Kurniawan, T.J. Lie, N. Idris, T. Kobayashi, H. Suyanto, T. Maruyama, K. Kagawa, M.O. Tjia, Hydrogen emission by Nd-YAG laser-induced shock wave plasma and its application to the quantitative analysis of zircalloy, J. Appl. Phys. 96 (2004) 1301–1309.
[36] K. Kagawa, N. Idris, M. Wada, K.H. Kurniawan, K. Tsuyuki, S. Miura, Carbon analysis for inspecting carbonation of concrete using TEA CO_2 laser-induced plasma, Appl. Spectrosc. 58 (2004) 887–896.
[37] K.H. Kurniawan, M. Pardede, R. Hedwig, Z.S. Lie, T.J. Lie, D.P. Kurniawan, M. Ramli, K. Fukumoto, H. Niki, S.N. Abdulmadjid, N. Idris, T. Maruyama, K. Kagawa, M.O. Tjia, Quantitative hydrogen analysis of zircalloy-4 using low-pressure laser plasma technique, Anal. Chem. 79 (2007) 2703–2707.
[38] A. Khumaeni, M. Ramli, Y. Deguchi, Y.I. Lee, N. Idris, K.H. Kurniawan, T.J. Lie, K. Kagawa, New technique for the direct analysis of food powders confined in a small hole using transversely excited atmospheric CO_2 laser-induced gas plasma, Appl. Spectrosc. 62 (2008) 1344–1348.
[39] A. Khumaeni, Z.S. Lie, H. Niki, K.H. Kurniawan, E. Tjoeng, Y.I. Lee, K. Kurihara, Y. Deguchi, K. Kagawa, Direct analysis of powder samples using transversely excited atmospheric CO_2 laser-induced gas plasma at 1 atm, Anal. Bioanal. Chem. 400 (2011) 3279–3287.
[40] L.I. Sedov, Similarity and Dimensional Methods in Mechanics, Academic Press, New York, 1959, p. 213.